

# Design, synthesis and biological evaluation of novel sulfamoyl benzamides as allosteric activators of human glucokinase

Prateek Sharma<sup>1,2</sup>, Anju Goyal<sup>1</sup>, Ajmer Singh Grewal<sup>3\*</sup>

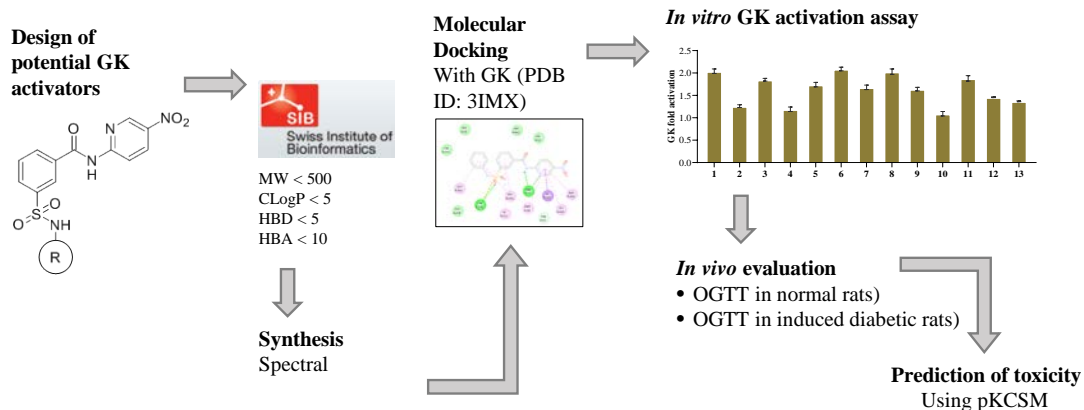
<sup>1</sup>Chitkara College of Pharmacy, Chitkara University, Punjab, India. <sup>2</sup>Government Pharmacy College, Rakkar, Himachal Pradesh, India.

<sup>3</sup>Guru Gobind Singh College of Pharmacy, Yamuna Nagar, Haryana, India

Submitted on: 17-Nov-2023, Accepted and Published on: 11-Jan-2024

Article

## ABSTRACT



Glucokinase (GK) activators, which target the GK enzyme, are an emerging class of therapeutics with promising effects against diabetes. The objective of this work was to create a new group of sulfamoyl benzamide derivatives with the ability to activate GK and evaluate their effectiveness in treating diabetes. From benzoic acid, several compounds containing sulfamoyl benzamide scaffold were synthesized and evaluated for their ability to activate GK in an *in vitro* enzymatic experiment. *In silico* docking analyses were employed to explore how the most suitable arrangements in the allosteric area of the GK enzyme interact during binding. The effectiveness of the identified substances in reducing high blood sugar levels was assessed using the oral glucose tolerance test (OGTT) in healthy rats. This evaluation was based on the results of laboratory tests on enzymes and *in silico* simulations. One of the most active compounds from the antihyperglycemic assay was then tested for its antidiabetic effects in an induced diabetic rat OGTT assay. The *in vitro* GK activation was best among compounds 1, 6, and 8 (activation fold: 2.03-2.09). In the OGTT assay (normal rats), compounds 1 and 6 showed promising antihyperglycemic activity. *In vivo* antidiabetic assay confirmed the consistency with *in silico* and *in vitro* outcomes. The newly synthesized derivatives of sulfamoyl benzamide have the potential to be used as a basis for the development of further GK activators that are both safe and efficacious and can be administered orally. These activators may be used as therapeutic agents to treat type 2 diabetes.

**Keywords:** Antidiabetic activity; Diabetes; Glucokinase; Allosteric GK activators; Sulfamoyl benzamides.

## INTRODUCTION

The International Diabetes Federation (IDF) has released new data analysis revealing that the worldwide population of persons with diabetes has surpassed 537 million, marking a 16% surge (equal to 74 million people) compared to the IDF's previous projections in 2019. According to the most recent IDF Diabetes Atlas, the worldwide occurrence of diabetes has already reached 10.5%, with over half (44.7%) of individuals remaining

undiagnosed. According to IDF forecasts, the number of individuals living with diabetes is expected to reach 783 million by 2045, which corresponds to one in eight persons. This would result in a 46% rise, which is more than double the projected population growth of 20% throughout the same timeframe. Aside from the mortality hazards related to COVID-19, it is anticipated that over 6.7 million individuals have died in 2021 as a result of diabetes or its consequences. This accounts for over 10% (12.2%) of total worldwide fatalities from various causes<sup>1</sup>. Diabetic individuals exhibit hyperglycemia, this condition is marked by high levels of glucose in the blood, either from inadequate insulin release or a compromised body's ability to use insulin efficiently. Despite the existence of several oral medications, both single-drug and combination treatments have proven insufficient to attain sustained control of blood glucose levels, mostly owing to

\*Corresponding Author: **Dr. Ajmer Singh Grewal**, Associate Professor, Guru Gobind Singh College of Pharmacy, Yamuna Nagar, Haryana, India  
Tel: +91-94167-00430  
Email: ajmergrewal2007@gmail.com



the potential dangers of hypoglycemia and severe adverse reactions. Consequently, the advancement of research in identifying targets and creating new chemical compounds for enhanced treatment has been expedited<sup>2-5</sup>. Type 1 diabetes mellitus constitutes around 5-10% of the total population affected by diabetes & it is characterized by a progressive decline in the production of insulin by the pancreatic  $\beta$ -cells. On the other hand, type 2 diabetes mellitus (T2DM), which constitutes around 90-95% of the total population with diabetes, is a chronic condition that affects how the body processes carbohydrates, resulting in impaired glucose breakdown and diminished insulin activity. Despite the availability of several treatment options for diabetes, no one medication that successfully attains sustained regulation of blood glucose levels in the majority of individuals with diabetes. Consequently, in modern times, the majority of physicians advocate initiating therapy with a combination of antidiabetic medications during the early stages of the condition<sup>6-7</sup>. An excessive amount of antidiabetic medication may result in a significant decrease in blood sugar levels, resulting in serious toxic consequences. In such cases, immediate medical intervention is often necessary. The scientific community is now prioritizing the development of novel, secure, and clinically distinct antidiabetic medicines that may be used as standalone medication treatments with enhanced effectiveness. Recent research has provided evidence that small-molecule glucokinase (GK) activators may have the potential to fill this void<sup>8</sup>. GK, an enzyme located within cells, catalysis the transformation of glucose into glucose-6-phosphate (G-6-P) by a phosphorylation reaction. When blood glucose levels are around 8.0 mM, GK activity hits 50% of its highest level. GK acts as a molecular sensor in pancreatic  $\beta$ -cells, establishing a connection between blood glucose levels and insulin production via complex signaling pathways, hence regulating glucose-stimulated insulin secretion (GSIR). GK serves an essential function in controlling how the body processes glucose, making it a potentially effective therapeutic target for people affected with type 2 diabetes mellitus. It is predominantly present in hepatic cells and pancreatic  $\beta$ -cells. In the pancreas, it manages glucose metabolism in the liver and significantly influences glucose-stimulated insulin release (GSIR). Additionally, GK regulates the secretion of glucagon-like peptide-1 and glucose-dependent insulinotropic peptides from gastrointestinal entero-endocrine cells. GK is kept inactive in the liver nucleus, controlled by the glucokinase regulatory protein (GKRP). GK activators are a novel group of potential drugs that target the GK enzyme and have hypoglycemic effects.<sup>9-10</sup> In recent years, a diverse range of compounds such as benzamide derivatives,<sup>10-18</sup> acetamides,<sup>19-20</sup> carboxamides,<sup>21</sup> acrylamides,<sup>22</sup> benzimidazoles,<sup>23</sup> quinazolines,<sup>24</sup> thiazoles,<sup>25</sup> pyrimidines<sup>26</sup> and urea derivatives<sup>27-28</sup> have been identified as promising activators of GK. Researchers have mostly concentrated their scientific endeavors on derivatives of benzamide as GK activators because of their particular binding style and orientation in the allosteric region. By incorporating various functional groups onto the phenyl ring and amide -NH, a diverse array of compounds may be created that have the potential to behave as GK activators. Our research has recently

reported and published new substituted benzamide compounds that can activate GK<sup>18, 29-30</sup>. Considering the crucial significance of GK activators in the treatment of T2DM and the diverse research discoveries, we attempted to design novel GK activators using the benzamide nucleus as a foundation. Strategic changes were made to the benzamide nucleus to selectively target strong hydrogen bonds and hydrophobic interactions with amino acid residues located in the GK protein's allosteric region. In addition, the synthesized compounds were specifically intended to have the ability to be absorbed and used by the body when taken orally, achieved by including functional groups such as sulphonamides into the benzamide structure.

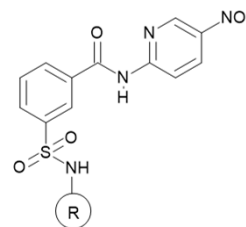


**Figure 1.** Markus structure of the designed sulfamoyl benzamides as potential GK activators.

## EXPERIMENTAL

All the chemicals, materials, solvents, and proteins needed for the study were purchased from SRL, Spectrochem, Sigma-Aldrich, Merck, S.D. Fine, LOBA, Fisher Scientific, & other places, and were used just as they were purchased. Using open capillary tubes and a Veego VMP-D melting point apparatus, the melting points were determined. The progress of the reaction was tracked using thin-layer chromatography (TLC) on silica gel-G plates. The compound's purity was confirmed by the presence of only one spot on the TLC plate. A Bruker make alpha 2 opus program was used to record infrared (IR) bands. The <sup>1</sup>H NMR and <sup>13</sup>C NMR spectra were collected on a Bruker Avance II NMR spectrophotometer using dimethyl sulfoxide (DMSO)-d<sub>6</sub> as a solvent. The findings are presented in parts per million ( $\delta$ , ppm), measured relative to tetramethylsilane (internal standard), and indicated as downfield values.

### *In silico* prediction of drug-likeness

The drug-likeness properties of the designed compounds (sulfamoyl benzamides) were computed using SwissADME web server (<http://www.swissadme.ch/>)<sup>31</sup>. Lipinski's rule of five<sup>32</sup> was used to assess their drug likeness.

### Synthesis

Dry benzoic acid (1 mmol) was placed in a flat bottom flask equipped with a magnetic stirrer, and the temperature was maintained at a constant level between 10 and 15 °C using a cold-water bath. With carefulness to prevent leakage, excess of chlorosulphonic acid (8.0 mL) was added to the flask. Once the acid had completely dissolved and the exothermic reaction subsided, the reaction flask was heated in a water bath at 70-80 °C for 2 hours to ensure completion of the reaction (observed by TLC on silica gel G). The contents of the flask were then cooled. The resulting mixture was poured into 150 g of crushed ice with

stirring to disperse lumps, and precipitates of 3-(chlorosulphonyl)benzoic acid were filtered under vacuum. The filtered product was washed with cold water and air-dried. The obtained product (1 mmol) was subjected to reflux with commercially available amines (1 mmol) in acetone until the reaction ceases. After cooling, precipitates of the respective sulphonamides were air-dried. The above prepared sulphonamides (1 mmol) were refluxed with thionyl chloride (1 mmol) for 3 hours, and excess thionyl chloride was distilled off to obtain the corresponding benzoyl chlorides. The benzoyl chlorides (1 mmol) obtained above were refluxed with 2-amino-5-nitropyridine (1.5 mmol) in acetone. The final products (benzamides) obtained after evaporating acetone were purified by recrystallization using ethyl alcohol.<sup>33-36</sup>

*3-[(2-Bromophenyl)sulfamoyl]-N-(5-nitropyridin-2-yl)benzamide (1)*: FTIR (cm<sup>-1</sup>): 3266.94, 3085.95, 2923.05, 1637.67, 1505.82, 1333.11, 1120.58, 1028.58, 829.48, 744.86; <sup>1</sup>H-NMR (δ ppm, 300 MHz): 9.06 (s, 1H, NH, CO-NH), 8.12-8.42 (m, 4H, 4CH, Benzoyl), 7.23 (s, 1H, NH, SO<sub>2</sub>-NH), 6.50-8.35 (m, 3H, 3CH, 5-NO<sub>2</sub>-Pyridin-2-yl), 7.10-7.64 (m, 4H, 4CH, 2-BrC<sub>6</sub>H<sub>4</sub>); <sup>13</sup>C-NMR (δ ppm, 100 MHz): 163.1 (C=O, CO-NH), 156.5 (C, C<sub>2</sub>, 5-NO<sub>2</sub>-Pyridin-2-yl), 146.0 (CH, C<sub>6</sub>, 5-NO<sub>2</sub>-Pyridin-2-yl), 140.0 (C, C<sub>3</sub>, C<sub>6</sub>H<sub>4</sub>), 136.5 (C, C<sub>5</sub>, 5-NO<sub>2</sub>-Pyridin-2-yl), 134.5 (C, C<sub>1</sub>, 2-BrC<sub>6</sub>H<sub>4</sub>), 134.2 (CH, C<sub>4</sub>, 5-NO<sub>2</sub>-Pyridin-2-yl), 133.4 (CH, C<sub>3</sub>, 2-BrC<sub>6</sub>H<sub>4</sub>), 131.5 (CH, C<sub>4</sub>, C<sub>6</sub>H<sub>4</sub>), 131.2 (CH, C<sub>6</sub>, C<sub>6</sub>H<sub>4</sub>), 130.1 (CH, C<sub>5</sub>, C<sub>6</sub>H<sub>4</sub>), 127.4 (CH, C<sub>5</sub>, 2-BrC<sub>6</sub>H<sub>4</sub>), 126.4 (CH, C<sub>4</sub>, 2-BrC<sub>6</sub>H<sub>4</sub>), 122.6 (CH, C<sub>6</sub>, 2-BrC<sub>6</sub>H<sub>4</sub>), 119.9 (CH, C<sub>2</sub>, C<sub>6</sub>H<sub>4</sub>), 115.5 (C, C<sub>2</sub>, 2-BrC<sub>6</sub>H<sub>4</sub>), 109.2 (CH, C<sub>3</sub>, 5-NO<sub>2</sub>-Pyridin-2-yl); HRMS (ESI TOF) m/z for C<sub>18</sub>H<sub>13</sub>BrN<sub>4</sub>O<sub>5</sub>S [M+H]<sup>+</sup>: Calculated: 476.986, Found: 475.1.

*3-(Ethylsulfamoyl)-N-(5-nitropyridin-2-yl)benzamide (2)*: FTIR (cm<sup>-1</sup>): 3391.69, 3114.07, 3114.07, 2923.32, 2923.32, 1694.46, 1646.27, 1646.27, 1516.02, 1516.02, 1392.61, 1330.74, 1250.88, 1170.53, 660.53; <sup>1</sup>H-NMR (δ ppm, 300 MHz): 8.90 (s, 1H, NH, CO-NH), 8.32-8.45 (m, 4H, 4CH, Benzoyl), 7.20 (t, 1H, NH, SO<sub>2</sub>-NH), 6.50-8.35 (m, 3H, 3CH, 5-NO<sub>2</sub>-Pyridin-2-yl), 2.22 (m, 2H, CH, CH<sub>2</sub>), 1.10 (t, 3H, CH, CH<sub>3</sub>).

*3-(Butylsulfamoyl)-N-(5-nitropyridin-2-yl)benzamide (3)*: FTIR (cm<sup>-1</sup>): 3355.66, 3115.85, 3115.85, 2922.36, 1694.77, 1634.37, 1634.37, 1558.78, 1467.61, 1331.87, 1282.95, 1116.21, 751.39; <sup>1</sup>H-NMR (δ ppm, 300 MHz): 8.89 (s, 1H, NH, CO-NH), 8.30-8.40 (m, 4H, 4CH, Benzoyl), 7.32 (t, 1H, NH, SO<sub>2</sub>-NH), 6.50-8.32 (m, 3H, 3CH, 5-NO<sub>2</sub>-Pyridin-2-yl), 2.65 (m, 2H, CH, CH<sub>2</sub>), 2.29 (m, 2H, CH, CH<sub>2</sub>), 2.30 (m, 2H, CH, CH<sub>2</sub>), 1.10 (t, 3H, CH, CH<sub>3</sub>).

*3-(Hydroxysulfamoyl)-N-(5-nitropyridin-2-yl)benzamide (4)*: FTIR (cm<sup>-1</sup>): 3614.22, 3328.20, 3113.50, 3113.50, 2923.67, 1749.26, 1676.38, 1518.14, 1352.36, 1240.02, 1134.27; <sup>1</sup>H-NMR (δ ppm, 300 MHz): 8.93 (s, 1H, NH, CO-NH), 8.30-8.42 (m, 4H, 4CH, Benzoyl), 7.26 (d, 1H, NH, SO<sub>2</sub>-NH), 6.50-8.30 (m, 3H, 3CH, 5-NO<sub>2</sub>-Pyridin-2-yl), 2.30 (d, 1H, NH-OH).

*3-(Hydrazinesulfonyl)-N-(5-nitropyridin-2-yl)benzamide (5)*: FTIR (cm<sup>-1</sup>): 3553.84, 3439.14, 3392.27, 2923.17, 1694.27, 1627.23, 1602.32, 1516.33, 1498.12, 1308.89, 1247.33, 1018.87, 737.51; <sup>1</sup>H-NMR (δ ppm, 300 MHz): 8.76 (s, 1H, NH, CO-NH), 8.30-8.41 (m, 4H, 4CH, Benzoyl), 7.21 (t, 1H, NH, SO<sub>2</sub>-NH),

6.50-8.30 (m, 3H, 3CH, 5-NO<sub>2</sub>-Pyridin-2-yl), 2.30 (d, 1H, NH, NH-NH<sub>2</sub>).

*N-(5-Nitropyridin-2-yl)-3-(phenylsulfamoyl)benzamide (6)*: FTIR (cm<sup>-1</sup>): 3399.03, 3157.46, 2923.22, 1679.77, 1631.33, 1600.45, 1549.81, 1452.82, 1417.64, 1337.67, 1119.98, 747.50; <sup>1</sup>H-NMR (δ ppm, 300 MHz): 8.97 (s, 1H, NH, CO-NH), 8.30-8.40 (m, 4H, 4CH, Benzoyl), 7.31 (s, 1H, NH, SO<sub>2</sub>-NH), 6.50-8.30 (m, 3H, 3CH, 5-NO<sub>2</sub>-Pyridin-2-yl), 7.15-7.60 (m, 5H, 5CH, C<sub>6</sub>H<sub>5</sub>); <sup>13</sup>C-NMR (δ ppm, 100 MHz): 165.0 (C=O, CO-NH), 133.5 (C, C<sub>1</sub>, C<sub>6</sub>H<sub>4</sub>), 120.5 (CH, C<sub>2</sub>, C<sub>6</sub>H<sub>4</sub>), 140 (C, C<sub>3</sub>, C<sub>6</sub>H<sub>4</sub>), 130.0 (CH, C<sub>4</sub>, C<sub>6</sub>H<sub>4</sub>), 129.0 (CH, C<sub>5</sub>, C<sub>6</sub>H<sub>4</sub>), 130.5 (CH, C<sub>6</sub>, C<sub>6</sub>H<sub>4</sub>), 156.5 (C, C<sub>2</sub>, 5-NO<sub>2</sub>-pyridin-2-yl), 110.5 (CH, C<sub>3</sub>, 5-NO<sub>2</sub>-pyridin-2-yl), 134.0 (CH, C<sub>4</sub>, 5-NO<sub>2</sub>-pyridin-2-yl), 135.0 (C, C<sub>5</sub>, 5-NO<sub>2</sub>-pyridin-2-yl), 145.0 (CH, C<sub>6</sub>, 5-NO<sub>2</sub>-pyridin-2-yl), 128.5 (C, C<sub>1</sub>, C<sub>6</sub>H<sub>5</sub>), 119.6 (CH, C<sub>2</sub>, C<sub>6</sub>H<sub>5</sub>), 130.1 (CH, C<sub>3</sub>, C<sub>6</sub>H<sub>5</sub>), 122.2 (CH, C<sub>4</sub>, C<sub>6</sub>H<sub>5</sub>), 129.2 (CH, C<sub>5</sub>, C<sub>6</sub>H<sub>5</sub>), 119.5 (CH, C<sub>6</sub>, C<sub>6</sub>H<sub>5</sub>); HRMS (ESI TOF) m/z for C<sub>18</sub>H<sub>14</sub>N<sub>4</sub>O<sub>5</sub>S [M+H]<sup>+</sup>: Calculated: 399.075, Found: 398.3.

*N-(5-Nitropyridin-2-yl)-3-sulfamoylbenzamide (7)*: FTIR (cm<sup>-1</sup>): 3735.90, 3390.87, 3278.24, 2925.70, 1662.20, 1582.89, 1572.78, 1528.00, 1461.36, 1343.13, 1216.75, 1166.67, 743.79; <sup>1</sup>H-NMR (δ ppm, 300 MHz): 8.88 (s, 1H, NH, CO-NH), 8.32-8.45 (m, 4H, 4CH, Benzoyl), 7.29 (s, 1H, NH, SO<sub>2</sub>-NH), 6.52-8.30 (m, 3H, 3CH, 5-NO<sub>2</sub>-Pyridin-2-yl).

*3-[(2-Chlorophenyl)sulfamoyl]-N-(5-nitropyridin-2-yl)benzamide (8)*: FTIR (cm<sup>-1</sup>): 3391.07, 3116.35, 2924.43, 1694.30, 1626.32, 1516.33, 1298.22, 1170.02, 834.63, 696.65; <sup>1</sup>H-NMR (δ ppm, 300 MHz): 8.79 (s, 1H, NH, CO-NH, Benzamide), 8.30-8.50 (m, 4H, 4CH, Benzoyl), 7.24 (s, 1H, NH, SO<sub>2</sub>-NH, Sulphonamide), 6.50-8.32 (m, 3H, 3CH, 5-NO<sub>2</sub>-Pyridin-2-yl), 7.06-7.56 (m, 4H, 4CH, 2-ClC<sub>6</sub>H<sub>4</sub>); <sup>13</sup>C-NMR (δ ppm, 100 MHz): 162.0 (C=O, CO-NH, Benzamide), 135 (C, C<sub>1</sub>, C<sub>6</sub>H<sub>4</sub>), 131.7 (CH, C<sub>2</sub>, C<sub>6</sub>H<sub>4</sub>), 129.0 (C, C<sub>3</sub>, C<sub>6</sub>H<sub>4</sub>), 130.5 (CH, C<sub>4</sub>, C<sub>6</sub>H<sub>4</sub>), 139.4 (CH, C<sub>5</sub>, C<sub>6</sub>H<sub>4</sub>), 119.9 (CH, C<sub>6</sub>, C<sub>6</sub>H<sub>4</sub>), 160.0 (C, C<sub>2</sub>, 5-NO<sub>2</sub>-Pyridin-2-yl), 110.0 (CH, C<sub>3</sub>, 5-NO<sub>2</sub>-Pyridin-2-yl), 132.2 (CH, C<sub>4</sub>, 5-NO<sub>2</sub>-Pyridin-2-yl), 135.2 (C, C<sub>5</sub>, 5-NO<sub>2</sub>-Pyridin-2-yl), 144 (CH, C<sub>6</sub>, 5-NO<sub>2</sub>-Pyridin-2-yl), 126.5 (C, C<sub>1</sub>, 2-ClC<sub>6</sub>H<sub>4</sub>), 126.0 (C, C<sub>2</sub>, 2-ClC<sub>6</sub>H<sub>4</sub>), 131.2 (CH, C<sub>3</sub>, 2-ClC<sub>6</sub>H<sub>4</sub>), 124.8 (CH, C<sub>4</sub>, 2-ClC<sub>6</sub>H<sub>4</sub>), 128.2 (CH, C<sub>5</sub>, 2-ClC<sub>6</sub>H<sub>4</sub>), 122.0 (CH, C<sub>6</sub>, 2-ClC<sub>6</sub>H<sub>4</sub>); HRMS (ESI TOF) m/z for C<sub>18</sub>H<sub>13</sub>ClN<sub>4</sub>O<sub>5</sub>S [M+H]<sup>+</sup>: Calculated: 433.125, Found: 432.6.

*N-(5-Nitropyridin-2-yl)-3-(propylsulfamoyl)benzamide (9)*: FTIR (cm<sup>-1</sup>): 3436.49, 3178.36, 2997.70, 2914.40, 1658.35, 1618.27, 1508.57, 1406.91, 1311.91, 1138.78, 699.26; <sup>1</sup>H-NMR (δ ppm, 300 MHz): 8.75 (s, 1H, NH, CO-NH, Benzamide), 8.30-8.42 (m, 4H, 4CH, Benzoyl), 7.38 (t, 1H, NH, SO<sub>2</sub>-NH), 6.50-8.32 (m, 3H, 3CH, 5-NO<sub>2</sub>-Pyridin-2-yl), 2.66 (m, 2H, CH, CH<sub>2</sub>, C<sub>3</sub>H<sub>7</sub>), 2.29 (m, 2H, CH, CH<sub>2</sub>, C<sub>3</sub>H<sub>7</sub>), 1.10 (t, 3H, CH, CH<sub>3</sub>, C<sub>3</sub>H<sub>7</sub>).

*3-[(2-Nitrophenyl)sulfamoyl]-N-(5-nitropyridin-2-yl)benzamide (10)*: FTIR (cm<sup>-1</sup>): 3363.87, 3270.30, 2923.04, 1678.26, 1633.20, 1593.77, 1504.10, 1334.81, 1290.80, 1164.09, 720.44; <sup>1</sup>H-NMR (δ ppm, 300 MHz): 8.85 (s, 1H, NH, CO-NH), 8.30-8.42 (m, 4H, 4CH, Benzoyl), 7.18 (s, 1H, NH, SO<sub>2</sub>-NH), 6.50-8.33 (m, 3H, 3CH, 5-NO<sub>2</sub>-Pyridin-2-yl), 7.05-7.55 (m, 4H, 4CH, 2-NO<sub>2</sub>-C<sub>6</sub>H<sub>5</sub>).

3-[(4-Nitrophenyl)sulfamoyl]-N-(5-nitropyridin-2-yl)benzamide (11): 3614.13, 2920.15, 1694.24, 1592.99, 1514.30, 1394.56, 1333.93, 1102.12, 738.43; <sup>1</sup>H-NMR ( $\delta$  ppm, 300 MHz): 8.75 (s, 1H, NH, CO-NH), 8.30-8.40 (m, 4H, 4CH, Benzoyl), 7.23 (s, 1H, NH, SO<sub>2</sub>-NH, Sulphonamide), 6.50-8.35 (m, 3H, 3CH, 5-NO<sub>2</sub>-Pyridin-2-yl), 7.10-7.60 (m, 4H, 4CH, 4-NO<sub>2</sub>-C<sub>6</sub>H<sub>5</sub>).

N-(5-Nitropyridin-2-yl)-3-(2-phenylhydrazinesulfonyl)benzamide (12): FTIR (cm<sup>-1</sup>): 3186.33, 3037.87, 2923.89, 2863.18, 1709.64, 1661.66, 1526.21, 1516.33, 1451.85, 1386.61, 1136.61, 746.90; <sup>1</sup>H-NMR ( $\delta$  ppm, 300 MHz): 8.72 (s, 1H, NH, CO-NH, Benzamide), 8.30-8.40 (m, 4H, 4CH, Benzoyl), 7.28 (d, 1H, NH, SO<sub>2</sub>-NH), 6.50-8.35 (m, 3H, 3CH, 5-NO<sub>2</sub>-Pyridin-2-yl), 7.10-7.60 (m, 5H, 5CH, C<sub>6</sub>H<sub>5</sub>).

3-(Benzylsulfamoyl)-N-(5-nitropyridin-2-yl)benzamide (13): FTIR (cm<sup>-1</sup>): 3493.34, 3362.75, 2923.24, 1712.45, 1632.10, 1591.36, 1552.98, 1494.68, 1469.98, 1331.59, 1282.43, 1128.07, 745.17; <sup>1</sup>H-NMR ( $\delta$  ppm, 300 MHz): 9.05 (s, 1H, NH, CO-NH, Benzamide), 8.29-8.42 (m, 4H, 4CH, Benzoyl), 7.24 (t, 1H, NH, SO<sub>2</sub>-NH, Sulphonamide), 6.50-8.28 (m, 3H, 3CH, 5-NO<sub>2</sub>-Pyridin-2-yl), 7.10-7.60 (m, 5H, 5CH, Benzyl), 3.30 (d, 2H, CH, CH<sub>2</sub>).

#### Enzymatic GK assay (*in vitro*)

The synthesized compounds underwent assessment for GK activity via spectrometry, employing a coupled reaction relating glucose-6-phosphate dehydrogenase. The reagents utilized in the assay were procured from Sigma-Aldrich and SRL. The preparation of each of the compounds was done using DMSO, and the analysis was carried out in a total volume of 2,000  $\mu$ L. This solution contained specific concentrations of many contents: 25 mM 2-(4-(2-hydroxyethyl) piperazine-1-yl)ethane sulfonic acid (HEPES, pH 7.4), 10 mM glucose, 25 mM potassium chloride, 1 mM magnesium chloride, 1 mM dithiothreitol, 1 mM adenosine triphosphate (ATP), 1 mM nicotinamide adenine dinucleotide (NAD), 2.5 U/mL G-6-PDH, 0.5  $\mu$ g GK, along with the synthesized compounds at a concentration of 10  $\mu$ M. The change in absorbance at a wavelength of 340 nm was observed throughout a 3-minute incubation time after initiating the reaction, serving as an indicator of the activity of the GK enzyme. The fold activation of the GK enzyme by the synthesized sulfamoyl benzamide derivatives was determined by comparing it to the control, where DMSO alone was considered to be 100% of GK activation.<sup>37-39</sup>

#### *In vivo* evaluation

Wister rats (weighing 150-200 g) were obtained from Lala Lajpat Rai University of Veterinary and Animal Sciences, Hisar (Haryana, India). The animals were housed in a regulated setting with ambient temperature and humidity levels maintained at 22  $\pm$  2  $^{\circ}$ C and 55  $\pm$  5%, respectively. All the animals experienced a 12-hour cycle of light and shade. Prior to the dietary modification, all the animals were given unrestricted access to the regular pellet food and water. This research was conducted in accordance with the guidelines and regulations established by the Committee for the Purpose of Control and Supervision of Experiments on Animals (CPCSEA), Government of India. Prior authorization was acquired from the Institutional Animal Ethics Committee

(IAEC) and the study was conducted under the approval number GGSCOP/IAEC/May2023/8.

#### OGTT (oral glucose tolerance test) in normal rats (anti-hyperglycemic study)

Based on the results of *in vitro* GK assay, three selected derivatives of 5-nitropyridine-2-yl benzamide (1, 6, and 8) were evaluated in OGTT in healthy rats. The rats were split up into five cohorts, with a total of six subjects in each of the groups. Before treatment, every single animal was fasted for a minimum of eight hours during the night. Group I served as the control group and administered with 0.5% CMC (p.o.). The metformin dosage for Group II was 30 mg/kg (p.o.). Groups III-V were given compounds 1, 6, and 8 at a dose of 50 mg/kg (p.o.). All groups received an oral dose of glucose (3 g/kg body weight) after 30 minutes of drug administration. Blood samples were collected from the tail vein before the administration of compounds as well as 0, 30, 60, 90, and 120 minutes following the administration of glucose. The serum glucose level was promptly assessed using a glucose measurement kit<sup>40</sup>. The area under the curve (AUC) for glucose was calculated by analyzing the blood glucose data collected throughout 0 to 2 hours.

#### OGTT assay in induced diabetic rats (antidiabetic study)

Based on the results of antihyperglycemic assay (OGTT in normal rats), best derivative (compound 6) was assessed for its antidiabetic activity using OGTT in induced diabetic rats. The rats were split into six distinct cohorts, with each group specifically composed of six individual rats. Before treatment, all animals had a fasting period of at least 8 hours. Animals were provided with a standard diet and water ad libitum. The subjects (rats) were kept in polyurethane enclosures under regulated conditions of room temperature and relative humidity, undergoing a regular 12-hour period of light followed by 12 hours of darkness. Hyperglycemia was induced in all fasted rats (except those in the normal control group) by injecting alloxan monohydrate, at a dosage of 150 mg/kg body weight (in normal saline, i.p.). After 72 hours, blood sugar amounts were assessed using a glucometer, and only rats displaying hyperglycemia were selected for subsequent study. The control groups, both normal and diabetic, were given only the vehicle (0.5% CMC solution, p.o.). The standard group was administered metformin (30 mg/kg body weight, orally), while the test groups received compound 6 at varying doses (25, 50, and 100 mg/kg body weight, p.o.). Every animal received a dose of glucose at 3 g/kg body weight (p.o.), precisely 30 minutes subsequent to the administration of the drug. Samples of blood were gathered from the tail vein of the animals before drug administration, as well as after 0, 2, 4, and 6 hours after glucose administration. Immediate measurement of serum glucose levels was performed using a glucometer and the glucose oxidase technique.<sup>41-42</sup>

#### *In-silico* docking study

AutoDock Vina was used to conduct *in-silico* docking analyses on the developed molecules within the GK protein's allosteric region<sup>43</sup> and the Windows 11-installed graphical user interface (AutoDock Tools)<sup>44</sup>. Marvin Sketch (ChemAxon) was

employed to generate the ligand's 2-D structures and then converted into three-dimensional structures using the Frog2 server<sup>45</sup>. Employing AutoDock Tools, the ligands were configured for docking. PDBQT files were generated utilizing the MOL format of the ligands. The information regarding the co-crystallized GK was obtained from the RCSB protein data bank, which can be accessed at the following URL: <http://www.rcsb.org/pdb>. After conducting a thorough assessment of numerous entries, the most ideal ligand-bound complex (PDB entry: 3IMX) was selected through a detailed examination of its three-dimensional structures. The complexed activator, all water molecules, and non-interacting ions were removed from the GK PDB file with the use of PyMOL (Schrodinger, LLC). The protein processing and creation of the PDBQT file from the PDB file were performed using AutoDock Tools. The macromolecule was docked by adding all the polar hydrogen atoms. The grid settings were determined through "Grid" function in AutoDock Tools. A configuration file named "conf.txt" was created and saved, presenting extensive information on the dimensions of the grid, characteristics of the protein and ligand, as well as the geometric properties of the search space. The dimensions of the grid were set to 30 × 30 × 30 XYZ points, with a grid spacing of 0.375 Å. The coordinates of the grid center were defined as (x, y, and z): 0.380, 2.721, and -16.334. The reliability of the docking method was assessed by docking the reference ligand into the active site of GK and subsequently correlating the resulting binding pose to that of the co-crystallized GK activator. Docking of the ligand molecules was carried out using AutoDock Vina after the ligand molecules had been optimized and prepared in PDBQT. The AutoDock scoring techniques were used to determine the rankings of the docked ligands. Following the docking process, the ligand posture demonstrating the most advantageous binding free energy ( $\Delta G$ ) was chosen. PyMOL & Discovery Studio (Dassault Systèmes) were used to conduct a more in-depth analysis of the hydrogen-bond interactions, the hydrophobic interactions, and any other aspects that were deemed to be important for the docked poses.

### In-silico prediction of ADMET

The optimized molecules underwent *in silico* evaluation to assess their pharmacokinetics and potential toxicity. This evaluation was performed utilizing the pkCSM web-based application.<sup>46-48</sup>

## RESULTS AND DISCUSSION

### In silico drug-likeness

The SwissADME online platform provides access to a comprehensive set of reliable prediction models, aiding in the prediction of physicochemical attributes, pharmacokinetic parameters, drug compatibility, and suitability for medicinal chemistry<sup>31</sup>. Given the constraints of time and cost associated with laboratory studies, *in silico* ADME (absorption, distribution, metabolism, and excretion) predictions were conducted to assess the potential of the lead chemicals. The success of a potential lead chemical in clinical trials depends on factors such as rapid absorption, uniform distribution across the body, efficient metabolism, and excretion without adverse side effects. "Drug-like" molecules often adhere to Lipinski's rule of five, which specifies criteria such as a molecular weight not exceeding 500, a logP value of 5 (milog), and a maximum of 10 hydrogen bond acceptors and 5 hydrogen bond donors. All designed compounds adhered to Lipinski's rule of five, as illustrated in Table 1. This compliance makes these compounds suitable candidates for further analysis to identify those meeting the specified criteria.<sup>32</sup> Table 1 indicates that while the majority of drugs exhibited a poor level of gastrointestinal absorption, they were found to be completely impermeable to the blood-brain barrier (BBB). Importantly, it was determined that all proposed compounds are not substrates of P-glycoprotein (PGP). The overexpression of P-glycoprotein (PGP) in the gastrointestinal tract can impede the uptake of drugs into blood capillaries, as PGP substrates are actively transported out of cells in the blood capillaries, the brain, and the gastrointestinal system. These findings contribute valuable insights into the potential pharmaceutical advancement of the studied compounds.

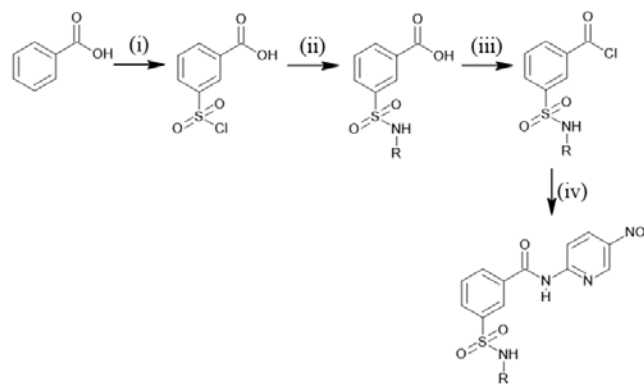
**Table 1.** Predicted chemical and physical characteristics of the designed sulfamoyl benzamide derivatives.

Compound	M.W.	NRB	HBA	HBD	TPSA (Å <sup>2</sup> )	Log P	Sol.	GI ab	BBB	PGP	Lipinski #
1	477.29	7	6	2	142.36	1.83	+	Low	No	No	0
2	350.35	7	7	2	142.36	0.67	++	Low	No	No	0
3	378.40	9	7	2	142.36	1.38	++	Low	No	No	0
4	338.30	6	8	3	162.59	0.36	++	Low	No	No	0
5	337.31	6	8	3	168.38	0.34	+++	Low	No	No	0
6	398.39	7	6	2	142.36	0.98	++	Low	No	No	0
7	322.30	5	7	2	156.35	0.43	++	Low	No	No	0
8	432.84	7	6	2	142.36	1.75	+	Low	No	No	0
9	364.38	8	7	2	142.36	0.97	++	Low	No	No	0
10	443.39	8	8	2	188.18	1.06	+	Low	No	No	1
11	443.39	8	8	2	188.18	0.76	++	Low	No	No	1
12	413.41	8	7	3	154.39	1.19	+	Low	No	No	0
13	412.42	8	7	2	142.36	1.65	++	Low	No	No	0

M.W.: Molecular weight; NRB: Number of rotatable bonds; HBA: Number of hydrogen bond acceptors; HBD: Number of hydrogen bond donors; TPSA: Topological polar surface area; Log P: Partition coefficient, Log  $P_{o/w}$  (iLOGP); Sol.: Solubility class (ESOL); +++: Very soluble; ++: Soluble, +: Moderately soluble; GI ab: Gastrointestinal absorption; BBB: Blood brain barrier penetration; PGP: Pgp substrate; Lipinski #: Number of violations to Lipinski's rule of five.

## Chemistry

The synthesis of the designed sulfamoyl benzamides is outlined in Scheme 1. To provide a succinct overview, the synthesis initiated with the chlorosulphonation of benzoic acid, resulting in the formation of 3-(chlorosulfonyl)benzoic acid. Subsequently, 3-(chlorosulfonyl)benzoic acid underwent reflux with commercially available amines, leading to the desired sulphonamides. The benzoyl chlorides, derived from refluxing of the aforementioned sulphonamides with thionyl chloride, were then subjected to refluxing with 2-amino-5-nitropyridine, culminating in the synthesis of the intended sulfamoyl benzamides. The final products were obtained with a satisfactory yield, as detailed in Table 2. Characterization of the synthesized compounds was performed using FTIR, <sup>1</sup>H-NMR, <sup>13</sup>C-NMR, and mass spectroscopy.



**Scheme 1.** Synthetic route for the preparation of various derivatives of sulfamoyl benzamide. **Reagents and Conditions:** (i) HSO<sub>3</sub>Cl, 80 °C, stirring, 2 h; (ii) NH<sub>2</sub>-R, acetone, reflux, 3-4 h; (iii) Thionyl chloride, acetone, reflux, 3-4 h; (iv) 2-Amino-5-nitropyridine, acetone, reflux, 3-4 h.

**Table 2.** Physical and chemical traits of the produced sulfamoyl benzamide derivatives.

S/N	R	Mol. Formula	M. Pt. (°C)	R <sub>f</sub> *	% Yield
1	-2-BrC <sub>6</sub> H <sub>4</sub>	C <sub>18</sub> H <sub>13</sub> BrN <sub>4</sub> O <sub>5</sub> S	166-167	0.75	51
2	-C <sub>2</sub> H <sub>5</sub>	C <sub>14</sub> H <sub>14</sub> N <sub>4</sub> O <sub>5</sub> S	144-145	0.68	63
3	-C <sub>4</sub> H <sub>9</sub>	C <sub>16</sub> H <sub>18</sub> N <sub>4</sub> O <sub>5</sub> S	147-149	0.56	45
4	-OH	C <sub>12</sub> H <sub>10</sub> N <sub>4</sub> O <sub>6</sub> S	155-156	0.55	56
5	-NH <sub>2</sub>	C <sub>12</sub> H <sub>11</sub> N <sub>5</sub> O <sub>5</sub> S	152-153	0.68	58
6	-C <sub>6</sub> H <sub>5</sub>	C <sub>18</sub> H <sub>14</sub> N <sub>4</sub> O <sub>5</sub> S	162-164	0.46	52
7	-H	C <sub>12</sub> H <sub>10</sub> N <sub>4</sub> O <sub>5</sub> S	151-152	0.59	63
8	-2-BrC <sub>6</sub> H <sub>4</sub>	C <sub>18</sub> H <sub>13</sub> ClN <sub>4</sub> O <sub>5</sub> S	163-164	0.60	54
9	-C <sub>3</sub> H <sub>7</sub>	C <sub>15</sub> H <sub>16</sub> N <sub>4</sub> O <sub>5</sub> S	145-147	0.63	50
10	-2-NO <sub>2</sub> C <sub>6</sub> H <sub>4</sub>	C <sub>18</sub> H <sub>13</sub> N <sub>5</sub> O <sub>7</sub> S	165-167	0.59	62
11	-4-NO <sub>2</sub> C <sub>6</sub> H <sub>4</sub>	C <sub>18</sub> H <sub>13</sub> N <sub>5</sub> O <sub>7</sub> S	168-170	0.75	58
12	-NHNHC <sub>6</sub> H <sub>5</sub>	C <sub>18</sub> H <sub>15</sub> N <sub>5</sub> O <sub>5</sub> S	156-158	0.45	52
13	-CHC <sub>6</sub> H <sub>5</sub>	C <sub>19</sub> H <sub>16</sub> N <sub>4</sub> O <sub>5</sub> S	165-167	0.67	59

\*TLC mobile phase: Toluene: Ethyl acetate (7:3).

The proton NMR spectra of the synthesized analogs exhibited a singlet signal at around  $\delta$  9.0 ppm, indicating the presence of one proton in the carboxamide (CONH) scaffold. This observation provides confirmation of the formation of a benzamide bond in all compounds. The presence of a singlet signal at approximately  $\delta$  7.20 ppm for one NH proton in the sulphonamide (SO<sub>2</sub>NH) group suggests the formation of sulphonamide derivatives through the reaction between the corresponding amines and sulphonyl chloride derivatives. In the  $\delta$  7.5-8.0 ppm range on the benzamide scaffold, the presence of a single signal (relating to C<sub>2</sub>), two doublet signals (relating to C<sub>4</sub> and C<sub>6</sub>), and a double doublet signal (relating to C<sub>5</sub>) confirms the meta positioning of the benzamide and sulphonamide functional groups relative to each other. In the <sup>1</sup>H-NMR spectra, two doublet signals and one singlet signal were observed, each accounting for three aromatic CH protons, detected around  $\delta$  6.8-8.0 ppm, affirming the synthesis of the intended derivatives through the reaction of benzoyl chloride with 2-amino-5-nitropyridine. Signals at approximately  $\delta$  165 ppm in the <sup>13</sup>C-NMR spectra further confirm the existence of the carbonyl (amide) bond, providing evidence for the formation of the benzamide linkage within these compounds. The FTIR spectra of these compounds displayed NH-vibrations (stretching) above 3500 cm<sup>-1</sup>, indicating

the presence of an amide. CH-stretching (aromatic) vibrations were observed above 3000 cm<sup>-1</sup>. Additionally, SO<sub>2</sub> stretching vibrations, both asymmetric and symmetric, were observed in the range of 1399-1301 cm<sup>-1</sup> and 1199-1101 cm<sup>-1</sup>, respectively. Peaks corresponding to SO<sub>2</sub>NH stretching were observed around 3399-3100 cm<sup>-1</sup>, confirming that these newly synthesized derivatives contain a sulphonamide (SO<sub>2</sub>NH) moiety and a benzamide functional group. Stretching vibrations for the carbonyl group were observed in the FTIR spectra within the range of 1699-1601 cm<sup>-1</sup>, indicating that these analogs contain a benzamide group in their structure.

### In vitro GK assay

The results obtained from the *in vitro* GK assay illustrate the extent to which the synthesized compounds activate the GK enzyme compared to the control (DMSO only), as depicted in Figure 2. Among the tested compounds, compounds 1, 6, and 8 showcased the most notable GK activity in the assay. These compounds demonstrated a GK activation fold ranging from 2.03 to 2.09 compared to the control. Compounds 3, 5, 7, 9, and 11 also displayed significant activations of GK, with fold activations ranging from 1.64 to 1.88. Meanwhile, compounds 12 and 13 exhibited a moderate level of GK activation, with a fold activation ranging from 1.37 to 1.46. On the other hand, compounds 2 and 4 demonstrated low GK activity, with a fold activation ranging from 1.19 to 1.26, in contrast to the control. Compound 10 did not yield favorable results in the *in vitro* GK experiment. Among the newly synthesized benzamide derivatives, molecule 6, which contains the N-phenyl sulphonamide group, exhibited the highest GK activity with a GK activation factor of 2.09. Compound 1, featuring a derivative containing an N-2-bromophenyl sulphonamide moiety, demonstrated a significant 2.04-fold increase in activation compared to the control. Similarly, compound 8, which includes a derivative with an N-2-chlorophenyl sulphonamide moiety, exhibited a noteworthy 2.03-fold increase in activation compared to the control.

## In vivo study

### OGTT assay in normal rats

After conducting an *in vitro* GK assay, compounds 1, 6, and 8 were identified for further assessment of their glucose-lowering potential using OGTT assay in normal rats, with metformin serving as the reference antidiabetic medication. The antihyperglycemic activity was evaluated by monitoring blood glucose concentrations (mg/dL) at different time intervals (Figure 3) and calculating the glucose Area Under the Curve (AUC) (Figure 4).

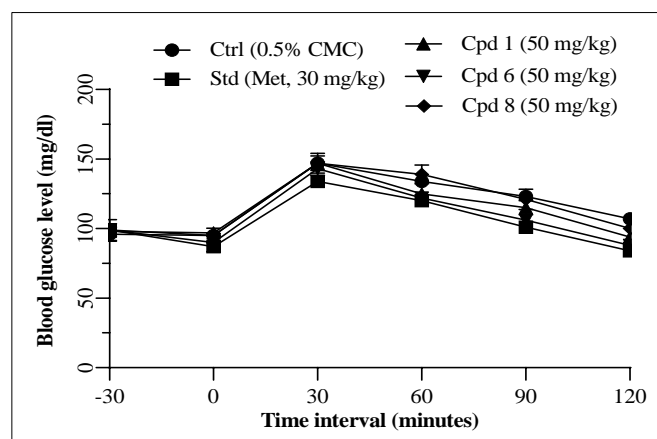


**Figure 3.** The effect of compounds 1, 6, and 8 on blood glucose levels in normal rat OGTT model. Results are presented as mean  $\pm$  SD (n = 6).

Results from the antihyperglycemic activity testing confirmed that compound 6 exhibited superior efficacy compared to compounds 1 and 8 in the OGTT experiment conducted on normal rats. Specifically, compound 6 demonstrated nearly equal potency to the standard medication (metformin) after 60 minutes, reaching a comparable reduction in blood glucose levels after 120 minutes. Moreover, compound 6 displayed a substantial

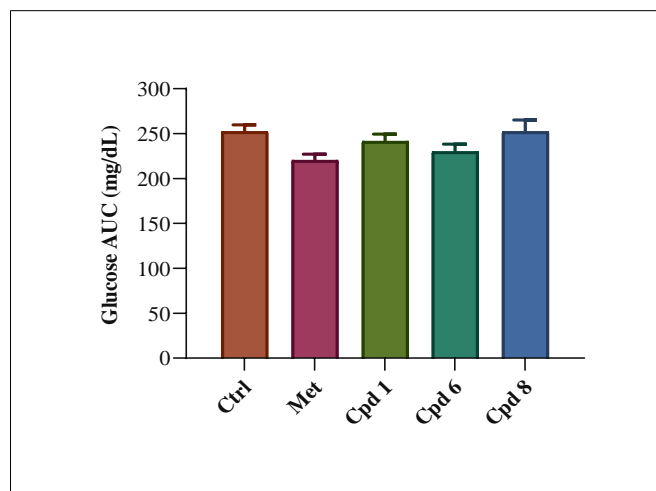


**Figure 4.** The reduction in glucose AUC displayed by compounds 1, 6, and 8 in OGTT (normal rats). Results are presented as mean  $\pm$  SD (n = 6).

decrease in glucose AUC, comparable to both the control and analogs, akin to metformin (standard). Notably, compounds 1, 6, and 8 steadily exhibited a trend of blood glucose reduction comparable to metformin. Of significance, compound 8 demonstrated notable efficacy in the *in vivo* experiment when juxtaposed with the conventional medicine metformin. Throughout the 120-minute duration of the OGTT, each compound exhibited a successful reduction of blood glucose levels to an acceptable range. Importantly, no hypoglycemic effects were observed during the entire assay period (0-20 minutes). These findings highlight the promising antihyperglycemic potential of compounds 1, 6, and 8, with compound 6 standing out as particularly effective in comparison to both the control and standard antidiabetic medication.

### OGTT assay in induced diabetic rats

In an OGTT assay conducted on alloxan-induced diabetic rats, compound 6 was evaluated for its anti-diabetic properties at doses of 25, 50, and 100 mg/kg body weight. Metformin, a commonly used antidiabetic medication, served as the reference. The anti-diabetic action was assessed by measuring glycemic concentration in blood (in mg/dl) at different timing intervals (Figure 5). Compound 6 exhibited increased activity with an escalating dose from 25 mg/kg to 100 mg/kg (body weight) at 2, 4, and 6-hour intervals. Notably, at a dose of 100 mg/kg (body weight), compound 6 demonstrated almost equal potency to the reference medication (metformin) at intervals of 2, 4, and 6 hours. This suggests a dose-dependent enhancement in anti-diabetic effects for this compound in the alloxan-induced diabetic rat model.

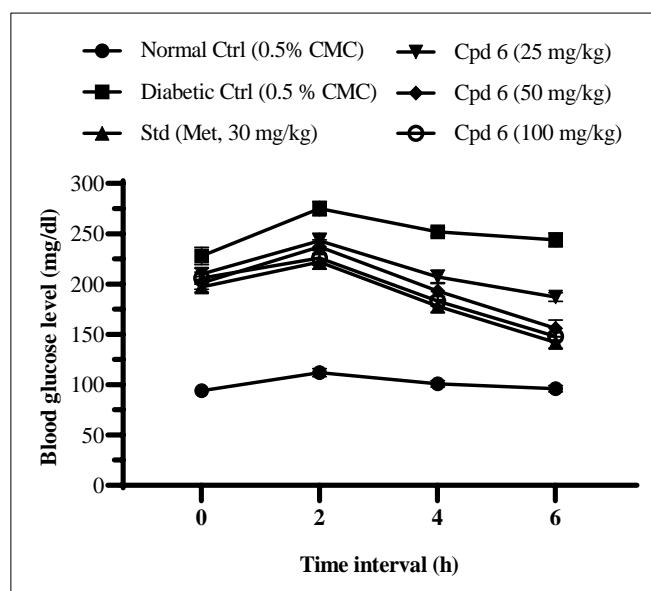


**Figure 5.** Effect of compound 6 on blood glucose levels at specified time intervals in induced diabetic rats OGTT. Results are presented as mean  $\pm$  SD (n = 6).

### In silico docking study

*In silico* virtual screening represents a practical approach in drug discovery and various scientific fields, offering a means to identify secure and efficient remedies for major diseases, including T2DM. This study utilized *in silico* molecular docking studies to explore the affinity and binding interactions of the proposed GK activators. AutoDock Vina was employed to investigate the allosteric site of GK (PDB ID: 3IMX). The docking methodology used in this study was validated by redocking a specific GK activator that had been previously co-crystallized into the allosteric site of GK. The re-docked GK activator generated a conformation closely matching the co-crystallized activator bound to the GK protein (Figure 6A), with a docking score ( $\Delta G$ , kcal/mol) of -10.8 (PDB ID: 3IMX), suggesting the use of a sound docking approach in this *in silico* investigation. The designed compounds were positioned within the allosteric site of human GK enzyme, interacting with specific residues including Arg63, Ser69, Tyr215, Met210, Tyr214, Val452, and Val455. Assessing the binding energy ( $\Delta G$ ) is crucial in identifying potential drug candidates for various ailments, where a lower binding energy indicates greater stability in the protein-ligand complex. A comparable binding pattern was observed in the allosteric region of the GK enzyme when the positioned design compounds were compared to the co-crystallized ligand (PDB ID: 3IMX) (Figure 6B). The molecular docking analyses suggested that these compounds exhibit a complementary conformation when bound to the allosteric site of the GK protein. The docking score ( $\Delta G$ ), along with the residues implicated in hydrogen bonding and hydrophobic interactions, are detailed in Table 3.

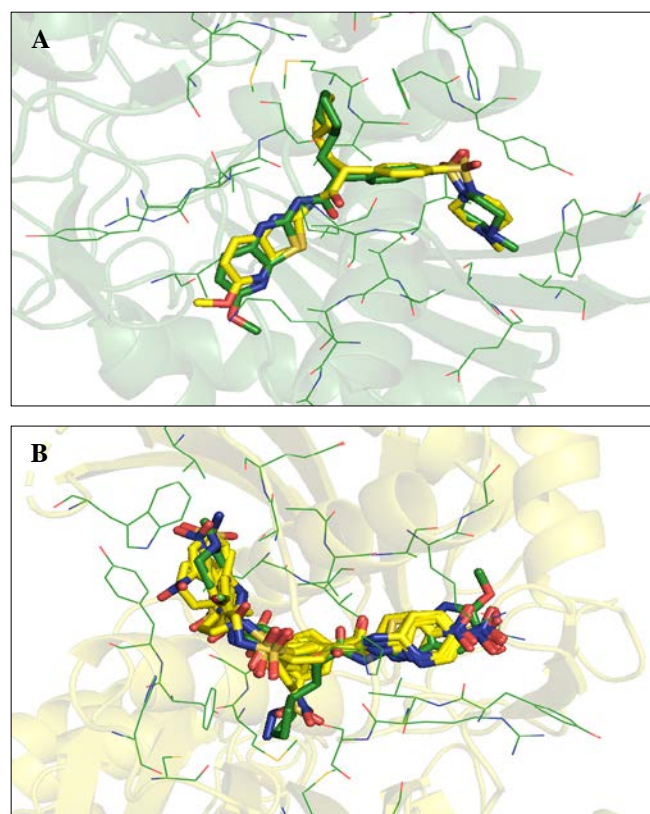


**Figure 6.** Redocking the co-crystallized GK activator served as validation for the docking process. A comparable position to the co-crystallized GK activator (green) was obtained with the re-docked ligand (yellow). B. Overlay of the co-crystallized GK activator (green) and the docked posture of the proposed ligands (yellow).

**Table 3.** The docking score ( $\Delta G$ ) and the residues responsible for the binding interactions between the designed compounds and the GK protein.

S/N	$\Delta G$	Hydrogen bonding		Hydrophobic interactions (residues involved)
		Residue	Distance (Å)	
1	-9.4	Arg63 Tyr214	2.27, 3.08 3.16	Pi-Sulfur (Tyr214), Pi-alkyl (Leu451, Val455, Ile211, Lys459, Pro66, Ala456), Pi-Sigma-Ile159
2	-8.0	Leu451 Arg63	2.38 Å 3.04 Å	Alkyl (Ala454, Leu451), Mixed Pi/Alkyl (Val455, Ile211, Pro66, Ala456, Ile159, Val62), Pi-sulfur (Tyr214)
3	-7.9	Arg49 Tyr188	3.16 3.30	Alkyl (Leu411), Mixed Pi/Alkyl (Arg49, Ile185, Val415, Try188, Ala416, Pro152), Pi-Sigma (Ile139), Carbon hydrogen (Tyr47)
4	-7.7	Leu451 Arg63	2.23 3.03	Pi-Sulfur (Tyr214), Pi-Alkyl (Ile211, Val455, Pro66, Ile159, Val62, Ala456), Carbon Hydrogen (Tyr61)
5	-7.5	Arg63	2.91 2.30	Pi-Sigma (Ile159), Pi-Sulfur (Tyr214), Pi-Alkyl (Val452, Val455, Ile211, Ala456, Lys459, Prp66)
6	-9.7	Arg63 Tyr214	2.22, 2.93 3.10	Pi-Sulfur (Tyr214), Pi-Alkyl (Val455, Leu451, Ile211, Pro66, Lys459, Ala456), Pi-Sigma (Ile159)
7	-7.8	Glu70 Ser69	2.58 2.30	Pi-Pi (Tyr215, Trp99), Pi-Alkyl (Ile211)
8	-9.7	Arg63 Tyr214	2.23, 2.96 3.12	Pi-Sulfur (Tyr214), Pi-Sigma (Ile159), Pi-Alkyl (Leu451, Val455, Ile211, Pro66, Lys459, Ala456)
9	-7.6	Arg63 Tyr214	3.14 3.23	Pi-Sigma (Ile159), Pi-Sulfur (Tyr214), Pi-Alkyl (Arg63, Ile211, Val455, Pro66, Lys459, Ala456)
10	-8.3	Trp99	2.93	Pi-Sulfur (Tyr214), Pi-Pi (Tyr215, Trp99), Pi-Alkyl (Val62, Pro66, Ile159, Ala456, Ile211, Val455, Tyr215, Ala454, Leu451)
11	-9.3	Ser69 Arg63	3.00 3.36	Pi-Sigma (Ile159, Val455), Pi-Sulfur (Tyr214), Pi-Pi (Tyr215, Trp99), Pi-Alkyl (Leu451, Lys459, Pro66, Ala456)
12	-9.0	Agr63	3.28	Pi-Alkyl (Leu451, Lys459, Pro66, Ala456, Val455, Ile211), Pi-Sigma-Ile159
13	-8.6	Arg63	3.20	Pi-Sigma (Ile159), Pi-Alkyl (Leu451, Lys459, Pro66, Ala456, Val455, Ile211)

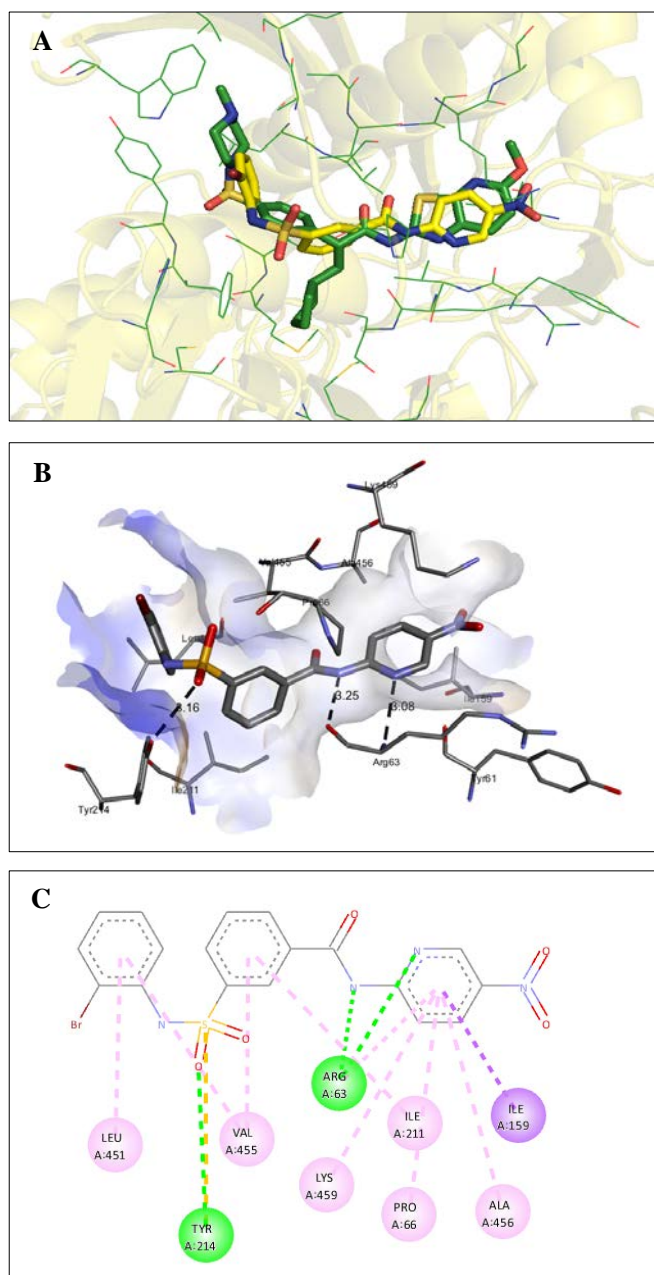


**Figure 7.** Interaction analysis of the compound 6 with GK. A. Overlay of the docked pose of compound 6 (yellow sticks) with that of the co-crystallized GK activator (green sticks). B. 3D docked pose of the compound 6 showing hydrogen bond interactions. C. 2D docked pose of compound 6 showing H-bonds (green dashes) and hydrophobic interactions (pink & purple dashes) with GK.

Compound 6 underwent a comprehensive analysis using PyMOL and Discovery Studio to investigate its interactions involving binding to the allosteric site residues of the GK protein (Figure 7). The docking conformation of compound 6 with the GK protein revealed three hydrogen bond interactions: the carbonyl group of the Arg63 of GK and the NH group of CONH (benzamide moiety) (bond distance: 2.22 Å), the NH group of Arg63 of GK and the N moiety of the 5-nitro pyridine-2-yl ring (2.93 Å), and the OH group of Tyr214 of GK and the S=O group of SO<sub>2</sub>NH (3.10 Å). Compound 6 demonstrated hydrophobic

interactions inside the allosteric site of GK, including Pi-Sulfur type (sulfur atom of SO<sub>2</sub>NH moiety with Try214 residue), Pi-alkyl type (phenyl moiety with Leu451 & Val455 residues, central phenyl ring with Ile211 & Val455 residues, and 5-nitro pyridine-2-yl ring with Arg63, Pro66, Ile211, Ala456 & Lys459 residues), and Pi-Sigma type (5-nitro pyridine-2-yl ring with Ile159 residue). These interactions provide insights into the molecular mechanisms through which compound 6 binds in the allosteric site of GK, supporting its potential as an allosteric activator of human GK.

#### **In-silico toxicity evaluation**

Using the pkCSM web-based application (Table 4), the pharmacokinetic characteristics and potential profiles for

**Table 4.** Predicted pharmacokinetics and toxicity for the optimized compounds generated using pkCSM.

Model name	Predicted value		
	1	6	8
<b>Absorption</b>			
Water solubility (log mol/L)	-4.528	-3.865	-4.48
Caco2 permeability (log Papp in 10 <sup>-6</sup> cm/s)	0.951	-0.54	0.95
Intestinal absorption (human) (% Absorbed)	86.313	85.255	86.577
Skin permeability (log Kp)	-2.741	-2.743	-2.742
P-Glycoprotein substrate (Yes/No)	Yes	Yes	Yes
P-Glycoprotein I inhibitor	Yes	Yes	Yes
P-Glycoprotein II inhibitor	Yes	Yes	Yes
<b>Distribution</b>			
VDss (human) (log L/kg)	-0.748	-0.672	-0.765
Fraction unbound (human)	0	0	0
BBB permeability	-1.194	-0.514	-1.186
CNS permeability	-2.458	-2.595	-2.481
<b>Metabolism</b>			
CYP2D6 substrate	No	No	No
CYP3A4 substrate	Yes	Yes	Yes
CYP1A2 inhibitor	Yes	Yes	Yes
CYP2C19 inhibitor	Yes	Yes	Yes
CYP2C9 inhibitor	Yes	Yes	Yes
CYP2D6 inhibitor	No	No	No
CYP3A4 inhibitor	Yes	Yes	Yes
<b>Excretion</b>			
Total clearance (log ml/min/kg)	-0.291	0.111	-0.049
Renal OCT2 substrate	No	No	No
<b>Toxicity</b>			
AMES toxicity	Yes	Yes	Yes
Maximum tolerated human dose (log mg/kg/day)	0.241	-0.03	0.241
hERG I inhibitor	No	No	No
hERG II inhibitor	Yes	Yes	Yes
Oral rat acute toxicity (LD <sub>50</sub> ) (mol/kg)	2.613	3.1	2.601
Oral rat chronic toxicity (log mg/kg_bw/day)	1.884	1.898	1.9
Hepatotoxicity	Yes	Yes	Yes
Skin sensitisation	No	No	No
<i>Tetrahymena pyriformis</i> toxicity (log ug/L)	0.316	0.321	0.317
Minnow toxicity (log mM)	0.357	0.817	0.503

carcinogenicity, mutagenicity, immunotoxicity, skin irritancy, & reproductive toxicity were compiled for the optimized compounds (1, 6, and 8). pkCSM is an openly accessible online tool that employs graph-based markers for the efficient assessment of pharmacokinetic and toxicity characteristics of small compounds<sup>46-48</sup>. The *in silico* evaluation indicated that these compounds exhibit favorable pharmacokinetic properties (ADME). Mutagenicity (AMES toxicity), hepatotoxicity, and cardiac toxicity (hERG II inhibition) were predicted for compounds 1, 6, and 8. The predicted values for oral rat acute toxicity were 2.6, 3.1, and 2.6 mol/kg for compounds 1, 6, and 8, respectively. Oral rat chronic toxicity was predicted to be 1.884, 1.898, and 1.90 log mg/kg\_bw/day for compounds 1, 6, and 8, respectively. A prior evaluation that is carried out *in silico* may be a useful supplement to future research on the potential dangers of compounds.

## CONCLUSION

In conclusion, this research article presents a comprehensive approach to drug discovery, employing *in silico* methods, chemical synthesis, and biological evaluations for a series of designed sulfamoyl benzamide derivatives considered as potential activators for GK enzyme in T2DM. The *in vitro* GK assay results indicated that compounds 1, 6, and 8 exhibited significant GK activation, with compound 6 showing the highest GK activity. Subsequent *in vivo* studies, including OGTT in normal rats and in alloxan induced diabetic rats, demonstrated the antihyperglycemic effects of these compounds. Notably, compound 6 displayed promising efficacy comparable to the standard antidiabetic drug metformin. The *in silico* docking study further supported the potential of the designed compounds as GK activators, revealing significant binding contacts in the allosteric location of the GK enzyme. Compound 6, with its hydrogen bond interactions and hydrophobic contacts, exhibited a robust binding pattern in the docking studies. Moreover, *in silico* toxicity evaluations predicted acceptable pharmacokinetic properties and suggested low toxicity profiles for compounds 1, 6, and 8. These findings provide a solid foundation for further exploration of these derivatives as potential candidates for the treatment of T2DM.

## ACKNOWLEDGMENTS

The authors are thankful to Chitkara College of Pharmacy, Chitkara University, Rajpura, Punjab (India) and CSIR- Institute of Himalayan Bioresource Technology, Palampur, Himachal Pradesh (India) for their support and encouragement for this research work.

## CONFLICT OF INTEREST STATEMENT

The authors declare that there is no conflict of interest for publication of this work.

## REFERENCES AND NOTES

- D.J. Magliano, E.J. Boyko. IDF Diabetes Atlas 10th edition scientific committee. IDF Diabetes Atlas [Internet]. 10th ed. International Diabetes Federation: Brussels, 2021.
- S. Dagogo-Jack. Diabetes Mellitus in Developing Countries and Underserved Communities. Springer International: Switzerland, 2016.
- A.S. Grewal, R. Kharb, D.N. Prasad, J.S. Dua, V. Lather. N-pyridin-2-yl benzamide analogues as allosteric activators of glucokinase: Design, synthesis, *in vitro*, *in silico* and *in vivo* evaluation. *Chem. Biol. Drug Des.* **2019**, 93, 364-372.
- P. Sharma, S. Singh, N. Sharma, D. Singla, K. Guarve, A.S. Grewal. Targeting human Glucokinase for the treatment of type 2 diabetes: an overview of allosteric Glucokinase activators. *J. Diabetes Metab. Disord.* **2022**, 21, 1129-1137.
- H. Fujieda, M. Kogami, M. Sakairi, N. Kato, M. Makino, N. Takahashi, T. Miyazawa, S. Harada, T. Yamashita. Discovery of a potent glucokinase activator with a favorable liver and pancreas distribution pattern for the treatment of type 2 diabetes mellitus. *Eur. J. Med. Chem.* **2018**, 156, 269-294.
- A. Arora, T. Behl, A. Sehgal, S. Singh, N. Sharma, S. Bhatia, E. Sobarzo-Sanchez, S. Bungau. Unravelling the involvement of gut microbiota in type 2 diabetes mellitus. *Life Sci.* **2021**, 273, 119311.
- S. Kumar, T. Behl, M. Sachdeva, A. Sehgal, S. Kumari, A. Kumar, G. Kaur, H.N. Yadav, S. Bungau. Implicating the effect of ketogenic diet as a preventive measure to obesity and diabetes mellitus. *Life Sci.* **2021**, 264, 118661.
- M. Pal. Recent advances in glucokinase activators for the treatment of type 2 diabetes. *Drug Discov. Today* **2009**, 14, 784-792.
- K.G. Alberti, P.Z. Zimmet. Definition, diagnosis and classification of diabetes mellitus and its complications. Part 1: diagnosis and classification of diabetes mellitus provisional report of a WHO consultation. *Diabetes Med.* **1998**, 15, 539-553.
- A.S. Grewal, V. Lather, N. Charaya, N. Sharma, S. Singh, V. Kairys. Recent developments in medicinal chemistry of allosteric activators of human glucokinase for type 2 diabetes mellitus therapeutics. *Curr. Pharm. Des.* **2021**, 26, 2510-2552.
- A.S. Grewal, B.S. Sekhon, V. Lather. Recent updates on glucokinase activators for the treatment of type 2 diabetes mellitus. *Mini Rev. Med. Chem.* **2014**, 14, 585-602.
- K.G. Pike, J.V. Allen, P.W. Caulkett, D.S. Clarke, C.S. Donald, M.L. Fenwick, K.M. Johnson, C. Johnstone, D. McKercher, J.W. Rayner, R.P. Walker. Design of a potent, soluble glucokinase activator with increased pharmacokinetic half-life. *Bioorg. Med. Chem. Lett.* **2011**, 21, 3467-3470.
- Y.Q. Li, Y.L. Zhang, S.Q. Hu, Y.L. Wang, H.R. Song, Z.Q. Feng, L. Lei, Q. Liu, Z.F. Shen. Design, synthesis and biological evaluation of novel glucokinase activators. *Chin. Chem. Lett.* **2011**, 22, 73-6.
- W. Mao, M. Ning, Z. Liu, Q. Zhu, Y. Leng, A. Zhang. Design, synthesis, and pharmacological evaluation of benzamide derivatives as glucokinase activators. *Bioorg. Med. Chem.* **2012**, 20, 2982-2991.
- L. Zhang, X. Chen, J. Liu, Q. Zhu, Y. Leng, X. Luo, H. Jiang, H. Liu. Discovery of novel dual-action antidiabetic agents that inhibit glycogen phosphorylase and activate glucokinase. *Eur. J. Med. Chem.* **2012**, 58, 624-639.
- K. Park, B.M. Lee, Y.H. Kim, T. Han, W. Yi, D.H. Lee, H.H. Choi, W. Chong, C.H. Lee. Discovery of a novel phenylethyl benzamide glucokinase activator for the treatment of type 2 diabetes mellitus. *Bioorg. Med. Chem. Lett.* **2013**, 23, 537-542.
- K. Park, B. Lee, K. Hyun, D. Lee, H. Choi, H. Kim, W. Chong, K. Kim, S. Nam. Discovery of 3-(4-methanesulfonylphenoxy)-N-[1-(2-methoxyethoxymethyl)-1H-pyrazol-3-yl]-5-(3-methylpyridin-2-yl)-benzamide as a novel glucokinase activator (GKA) for the treatment of type 2 diabetes mellitus. *Bioorg. Med. Chem.* **2014**, 22, 2280-2293.
- R. Singh, V. Lather, D. Pandita, V. Judge, K. N. Arumugam, A.S. Grewal. Synthesis, docking and antidiabetic activity of some newer benzamide derivatives as potential glucokinase activators. *Letts. Drug Des. Discov.* **2017**, 14, 540-53.
- Z.S. Chervallath, S.L. Gwaltney II, M. Sabat, M. Tang, J. Feng, H. Wang, J. Miura, P. Guntupalli, A. Jennings, D. Hosfield, B. Lee. Design, synthesis and SAR of novel glucokinase activators. *Bioorg Med Chem Lett.* **2013**, 23, 2166-2171.
- J. Pfefferkorn, A. uzman-Perez, J. Pettersen, M.L. Minich, K.J. Filipski, C.S. Jones, M. Tu, G. Aspnes. Discovery of (S)-6-(3-cyclopentyl-2-(4-

- (trifluoromethyl)-1H-imidazol-1-yl)propanamido)nicotinic acid as a hepatoselective glucokinase activator clinical candidate for treating type 2 diabetes mellitus. *J. Med. Chem.* **2012**, *55*, 1318-1333.
21. J.A. Pfefferkorn, M. Tu, K.J. Filipinski, A. Guzman-Perez, J. Bian, G.E. Aspnes, M.F. Sammons, W. Song, J.C. Li, C.S. Jones, L. Patel. The design and synthesis of indazole and pyrazolopyridine based glucokinase activators for the treatment of type 2 diabetes mellitus *Bioorg. Med. Chem. Lett.* **2012**, *22*, 7100-7105.
  22. A. Sidduri, J.S. Grimsby, W.L. Corbett, R. Sarabu, J.F. Grippo, J. Lou, R.F. Kester, M. Dvorozniak, L. Marcus, C. Spence, J.K. Racha. 2,3-Disubstituted acrylamides as potent glucokinase activators. *Bioorg. Med. Chem. Lett.* **2010**, *20*, 5673-5676.
  23. M. Ishikawa, K. Nonoshita, Y. Ogino, Y. Nagae, D. Tsukahara, H. Hosaka, S. Ohyama, Y. Nagata. Discovery of novel 2-(pyridine-2-yl)-1H-benzimidazole derivatives as potent glucokinase activators. *Bioorg. Med. Chem. Lett.* **2009**, *19*, 4450-4454.
  24. T. Iino, Y. Sasaki, M. Bamba, M. Mitsuya, A. Ohno, K. Kamata, H. Hosaka, H. Maruki, M. Futamura, R. Yoshimoto, S. Ohyama. Discovery and structure-activity relationships of a novel class of quinazoline glucokinase activators. *Bioorg. Med. Chem. Lett.* **2009**, *19*, 5531-5538.
  25. R.J. Hinklin, S.A. Boyd, M.J. Chicarelli. Identification of a new class of glucokinase activators through structure-based design. *J. Med. Chem.* **2013**, *56*, 7669-7678.
  26. K.J. Filipinski, A.G. uzman-Perez, J. Bian, C. Perreault, G.E. Aspnes, M.T. Didiuk, R.L. Dow, R.F. Hank, C.S. Jones, R.J. Maguire, M. Tu. Pyrimidone-based series of glucokinase activators with alternative donor-acceptor motif. *Bioorg. Med. Chem. Lett.* **2013**, *23*, 4571-4578.
  27. Y. Li, K. Tian, A. Qin, L. Zhang, H. Song, Z. Feng. Discovery of novel urea derivatives as dual-target hypoglycemic agents that activate glucokinase and PPAR $\gamma$ . *Eur. J. Med. Chem.* **2014**, *182*-192.
  28. L. Zhang, K. Tian, Y. Li, L. Lei, A. Qin, L. Zhang, H. Song, L. Huo, L. Zhang, X. Jin, Z. Shen. Novel phenyl-urea derivatives as dual-target ligands that can activate both GK and PPAR $\gamma$ . *Acta Pharm. Sin. B* **2012**, *2*, 588-97.
  29. S. Singh, S. Arora, E. Dhalio, N. Sharma, K. Arora, A.S. Grewal. Design and synthesis of newer N-benzimidazol-2yl benzamide analogues as allosteric activators of human glucokinase. *Med. Chem. Res.* **2021**, *30*, 760-770.
  30. S. Arora, A.S. Grewal, N. Sharma, K. Arora, E. Dhalio, S. Singh. Design, synthesis, and evaluation of some novel N-benzothiazol-2-yl benzamide derivatives as allosteric activators of human glucokinase. *J. Appl. Pharm. Sci.* **2021**, *11*, 038-047.
  31. A. Daina, O. Michielin, V. Zoete. SwissADME: a free web tool to evaluate pharmacokinetics, drug-likeness and medicinal chemistry friendliness of small molecules. *Sci. Rep.* **2017**, *7*, 42717.
  32. C.A. Lipinski, F. Lombardo, B.W. Dominy, P.J. Feeney. Experimental and computational approaches to estimate solubility and permeability in drug discovery and development settings. *Adv. Drug Deliv. Rev.* **2001**, *46*, 3-26.
  33. R. Singh, V. Lather, D. Pandita, V. Judge, K. N. Arumugam, A.S. Grewal. Synthesis, docking and antidiabetic activity of some newer benzamide derivatives as potential glucokinase activators. *Lett. Drug Des. Discov.* **2017**, *14*, 540-53.
  34. N. Charaya, D. Pandita, A.S. Grewal, V. Lather. Design, synthesis and biological evaluation of novel thiazol-2-yl benzamide derivatives as glucokinase activators. *Comput. Biol. Chem.* **2018**, *73*, 221-229.
  35. A.S. Grewal, V. Lather, D. Pandita, G. Bhayana. Synthesis, docking and evaluation of phenylacetic acid and trifluoro-methylphenyl substituted benzamide derivatives as potential PPAR delta agonists. *Lett. Drug Des. Discov.* **2017**, *14*, 1239-51.
  36. A.S. Grewal, R. Kharb, D.N. Prasad, J.S. Dua, V. Lather. Design, synthesis and evaluation of novel 3,5-disubstituted benzamide derivatives as allosteric glucokinase activators. *BMC Chem.* **2019**, *13*, 2.
  37. K.A. Mookhtiar, S.S. Kalinowski, K.S. Brown, Y.H. Tsay, C. Smith-Monroy, G.W. Robinson. Heterologous expression and characterization of rat liver glucokinase regulatory protein. *Diabetes* **1996**, *45*, 1670-1677.
  38. A.M. Efanov, D.G. Barrett, M.B. Brenner, S.L. Briggs, A. Delaunoy, J.D. Durbin, U. Giese, H. Guo, M. Radloff, G.S. Gil, S. Sewing. A novel glucokinase activator modulates pancreatic islet and hepatocyte function. *Endocrinology* **2005**, *146*, 3696-3701.
  39. M. Futamura, H. Hosaka, A. Kadotani, H. Shimazaki, K. Sasaki, S. Ohyama, T. Nishimura, J.I. Eiki, Y. Nagata. An allosteric activator of glucokinase impairs the interaction of glucokinase and glucokinase regulatory protein and regulates glucose metabolism. *J. Biol. Chem.* **2006**, *281*, 37668-37674.
  40. M.F. Ahmed, S.M. Kazim, S.S. Ghorri, S.S. Mehjabeen, S.R. Ahmed, S.M. Ali, M. Ibrahim. Antidiabetic activity of Vinca rosea extracts in alloxan-induced diabetic rats. *Int. J. Endocrinol.* **2010**, 841090.
  41. A. Chauhan, A.S. Grewal, D. Pandita, V. Lather. Novel Cinnamic Acid Derivatives as Potential PPAR $\delta$  Agonists for Metabolic Syndrome: Design, Synthesis, Evaluation and Docking Studies. *Curr. Drug Discov. Technol.* **2020**, *17*, 338-347.
  42. N. Charaya, D. Pandita, A.S. Grewal, V. Lather. Design, synthesis and biological evaluation of novel thiazol-2-yl benzamide derivatives as glucokinase activators. *Comput. Biol. Chem.* **2018**, *73*, 221-229.
  43. O. Trott, A.J. Olson. AutoDock Vina: improving the speed and accuracy of docking with a new scoring function, efficient optimization, and multithreading. *J. Comput. Chem.* **2010**, *31*, 455-461.
  44. G.M. Morris, R. Huey, W. Lindstrom, M.F. Sanner, R.K. Belew, D.S. Goodsell, A.J. Olson. AutoDock4 and AutoDockTools4: Automated docking with selective receptor flexibility. *J. Comput. Chem.* **2009**, *30*, 2785-2791.
  45. M.A. Miteva, F. Guyon, P. Tufféry. Frog2: Efficient 3D conformation ensemble generator for small compounds. *Nucleic Acids Res.* **2010**, *38*, W622-W627.
  46. D.E. Pires, L.M. Kaminskis, D.B. Ascher. Prediction and optimization of pharmacokinetic and toxicity properties of the ligand. *Methods Mol. Biol.* **2018**, *1762*, 271-284.
  47. S. Kamboj, M. Mukhija, J. Monga, R. Singla, J. Chaudhary. Mechanistic investigation of Quercetin in the management of complications of Diabetes mellitus by Network Pharmacology. *J. Mol. Chem.* **2023**, *4* (1 SE-Medicinal Chemistry), 684.
  48. A.C. Salgueiro, V. Folmer, H.S. da Rosa, M.T. Costa, A.A. Boligon, F.R. Paula, D.H. Roos, G.O. Puntel. In vitro and in silico antioxidant and toxicological activities of Achyrocline satureioides. *J. Ethnopharmacol.* **2016**, *194*, 6-14.